

High-Order Spectral Volume Method for the Navier-Stokes Equations on Unstructured Grids

Yuzhi Sun* and Z.J. Wang†

Department of Mechanical Engineering, Michigan State University, East Lansing, MI 48824

In this paper, the spectral volume (SV) method is extended to solve the Navier-Stokes equations by treating the viscous terms with a mixed formulation named local Discontinuous Galerkin approach. The SV method combines two key ideas, which are the basis of the finite volume and the finite element methods, i.e., the physics of wave propagation accounted for by the use of a Riemann solver and high-order accuracy achieved through high-order polynomial reconstructions within spectral volumes. The formulation of the SV method for the two-dimensional compressible Navier-Stokes equations is described. Accuracy studies are performed on the scalar advection diffusion and the Navier-Stokes equations using problems with analytical solutions. It is shown that the designed order of accuracy is achieved for all orders of polynomial reconstructions. The solver is then used to solve other viscous laminar flow problems to shown its potential.

I. Introduction

The spectral volume (SV) method¹⁻⁴ is a recently developed high-order finite volume method for hyperbolic conservation laws. It has been successfully demonstrated for multi-dimensional Euler equations. The SV method is a Godunov-type finite volume method⁵, which has been under development for several decades, and has become the state-of-the-art for the numerical solution of hyperbolic conservation laws. For a review of the literature on the Godunov-type method, refer to Reference 1, and the references therein. The SV method is also related to the discontinuous Galerkin (DG) method⁶, and high-order element or SV-wise polynomials are used to approximate the state variables. Similar to the Godunov-type method, the SV method has two key components. One is data reconstruction, and the other is the (approximate) Riemann solver. What distinguishes the SV method from the traditional high-order k-exact finite volume method⁷ and the weighted essentially non-oscillatory (WENO) method⁸⁻¹⁰ is the data reconstruction. Instead of using a (large) stencil of neighboring cells to perform a high-order polynomial reconstruction, a simplex unstructured grid cell – called a spectral volume – is partitioned into a “structured” set of sub-cells called control volumes (CVs), and cell-averaged solutions on these sub-cells are then the degrees-of-freedom (DOFs). These DOFs are used to reconstruct a high order polynomial inside the SV. If all the spectral volumes are partitioned in a geometrically similar manner, a universal reconstruction formula can be obtained for all simplexes. With reconstructed solutions at both sides of an interface, the numerical flux can be computed with an approximate Riemann solver. Then the DOFs can be updated to high-order accuracy using the usual Godunov-type finite volume method.

Comparisons between the DG and SV methods have been made recently¹¹⁻¹². The SV method avoids the volume integral required in the DG method. However, it does introduce more interfaces where more Riemann problems are solved. For 2D Euler equations, both methods seem to achieve similar efficiency¹¹. Both the DG and SV methods are capable of achieving the optimal order of accuracy. The DG method usually has a lower error magnitude, but the SV method allows larger time steps. Due to its inherent property of subcell resolution, the SV method is capable of capturing discontinuities with a higher resolution than the DG method.

Ultimately, we wish to extend the SV method to the Navier-Stokes equations to perform large eddy simulation and direct numerical simulation of turbulent flow for problems with complex geometries. To achieve this goal, we first must find a technique to properly discretize the second order viscous terms. In the second-order finite volume method, the solution gradients at an interface are usually computed by averaging the gradients of the neighboring

* Graduate Student (sunyuzhi@egr.msu.edu), AIAA Student Member

† Associate Professor (zjw@egr.msu.edu), AIAA Associate Fellow

cells sharing the face. For higher-order elements, special care has to be taken in computing the solution gradients. For example, Cockburn and Shu developed the so-called local discontinuous Galerkin method (LDG) to treat the second order viscous terms and proved stability and convergence with error estimates¹³ motivated by the successful numerical experiments of Bassi and Rebay¹⁴. Baumann and Oden¹⁵, Oden, Babuska and Baumann¹⁶ introduced various penalty-type methods for the discretization of second order viscous terms. Riviere, Wheeler and Girault¹⁷ analyzed three discontinuous Galerkin approximations for solving elliptic problems in two or three dimensions. More recently, Shu¹⁸ summarized three different formulations for the diffusion equation, and Zhang and Shu¹⁹ performed a Fourier type analysis for these three formulations.

Recently several formulations based on the successful LDG and penalty-type approaches have been developed and analyzed for the SV method using the 1D pure diffusion equation²⁰. Three SV formulations, i.e. naïve formulation, local SV (LSV) and penalty SV (PSV) approaches, are tested. It was found that the naïve formulation converges to the wrong solution, while the LSV and the PSV approaches are consistent, stable and convergent. It was shown that the LSV method achieved the optimal order of accuracy, i.e., (k+1)th order for degree k polynomial reconstructions. The PSV approach, however, achieved only kth order accuracy if k is even. Therefore, the LSV approach is selected for the extension to the Navier-Stokes equations. Before we attempt to solve the full Navier-Stokes equations, the LSV formulation is further tested on 1D (both linear and non-linear) and 2D convection-diffusion equations.

The paper is therefore organized as follows. In Section 2, we describe the spectral volume formulation for the 2D convection-diffusion equation. The degeneration from 2D to 1D should be obvious. After that, the extension of the SV method to the Navier-Stokes equations is presented in Section 3. Section 4 presents accuracy studies for both the convection-diffusion and Navier-Stokes equations. In addition, other computations of laminar flow are carried out, and results are compared with benchmark results. Finally, conclusions and some possible future work are summarized in section 5.

II. Spectral Volume Formulation for 2D Convection-Diffusion Equation

For the sake of simplicity, the following 2D convection-diffusion equation is considered first in domain Ω with proper initial and boundary conditions

$$\frac{\partial u}{\partial t} + \nabla \cdot (\boldsymbol{\beta}u) - \nabla \cdot (\mu \nabla u) = 0, \quad (2.1)$$

where $\boldsymbol{\beta}$ is the convective velocity vector and μ is the diffusion coefficient. The domain Ω is discretized into N non-overlapping triangular cells. These cells are called spectral volumes (SVs) in the SV method, i.e., $\Omega = \bigcup_{i=1}^N S_i$. A SV is first partitioned into a set of structured subcells called control volumes (CVs) depending on the degree of the reconstruction polynomial. The partitions to be used in this paper are shown in Figure 1 for various degrees of reconstruction. The degrees-of-freedom (DOFs) in the SV method are the subcell-averages of the state variable. Let the j -th CV of S_i be denoted by $C_{i,j}$. Following the local DG (LDG) approach^{13,14,21}, we define an auxiliary variable,

$$q = \nabla u. \quad (2.2)$$

Then Eq. (2.1) becomes

$$\frac{\partial u}{\partial t} + \nabla \cdot (\boldsymbol{\beta}u) - \nabla \cdot (\mu q) = 0. \quad (2.3)$$

Integrating (2.2) and (2.3) in $C_{i,j}$ and performing integration by parts, we obtain

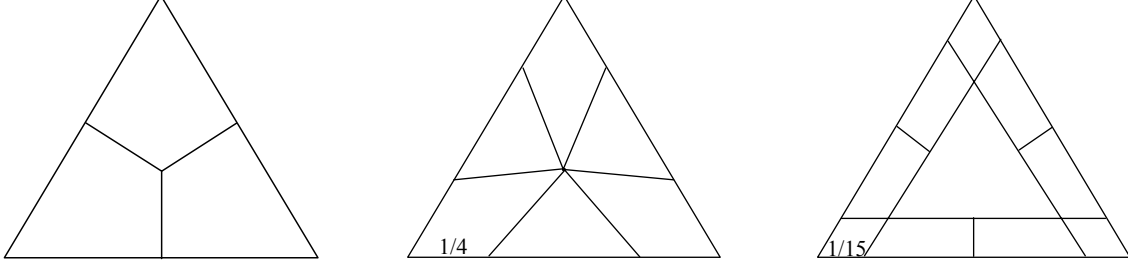


Figure 1. Linear, quadratic and cubic partitions

$$\bar{q}_{i,j} V_{i,j} = \sum_{r=1}^K \int_{A_r} u \mathbf{n} dA \quad (2.4)$$

$$\frac{d\bar{u}_{i,j}}{dt} V_{i,j} + \sum_{r=1}^K \int_{A_r} \beta \mathbf{u} \cdot \mathbf{n} dA - \sum_{r=1}^K \int_{A_r} \mu q \cdot \mathbf{n} dA = 0 \quad (2.5)$$

where $\bar{q}_{i,j}$ and $\bar{u}_{i,j}$ are the CV-averaged gradient and solution in $C_{i,j}$, K is the number of faces in $C_{i,j}$, and A_r represents the r -th face of $C_{i,j}$ and \mathbf{n} is the unit surface normal. Since the solution u is SV-wise continuous, u and q at SV boundaries are not well defined, and so they are replaced with the so-called “numerical fluxes” \hat{u} , \tilde{u} and \hat{q} , i.e.,

$$\bar{q}_{i,j} V_{i,j} = \sum_{r=1}^K \int_{A_r} \hat{u} \mathbf{n} dA, \quad (2.6)$$

$$\frac{d\bar{u}_{i,j}}{dt} V_{i,j} + \sum_{r=1}^K \int_{A_r} \beta \tilde{u} \cdot \mathbf{n} dA - \sum_{r=1}^K \int_{A_r} \mu \hat{q} \cdot \mathbf{n} dA = 0. \quad (2.7)$$

For the inviscid flux, one can use an approximate Riemann solver such as the Roe Riemann solver. In the scalar case, Roe flux degenerates to the following upwind flux

$$\tilde{u} = \begin{cases} u_L & \beta \cdot \mathbf{n} > 0 \\ u_R & \beta \cdot \mathbf{n} < 0 \end{cases} \quad (2.8)$$

The other two numerical fluxes are defined by alternating the direction in the following manner

$$\begin{aligned} \hat{u} &= u_L \\ \hat{q} &= q_R \end{aligned} \quad (2.9)$$

or

$$\begin{aligned} \hat{u} &= u_R \\ \hat{q} &= q_L. \end{aligned} \quad (2.10)$$

Other aspects of the SV method are already described in the earlier papers¹⁻⁴, and details are not given here. For example, given the DOFs, the reconstructed polynomial $p_i(x, y)$ can be conveniently expressed as

$$p_i(x, y) = \sum_{j=1}^m L_{i,j}(x, y) \bar{u}_{i,j}, \quad (2.11)$$

where $L_j(x, y) \in P^{k-1}$ are the "shape" functions, which are given in Reference 2. All the surface integrals in (2.6) and (2.7) are performed with Gauss quadrature formulas. For time integration, we use the three-stage TVD Runge-Kutta scheme⁶.

III. Extension to the Navier-Stokes Equations

With the description given for the convection-diffusion equation, the extension to the Navier-Stokes is straightforward. We consider the two-dimensional Navier-Stokes equations written in the conservation form

$$\frac{\partial Q}{\partial t} + \nabla \cdot \bar{F}_e(Q) - \nabla \cdot \bar{F}_v(Q, \nabla Q) = 0 \quad (3.1a)$$

where the conservative variables Q and the Cartesian components $f_e(Q)$ and $g_e(Q)$ of the inviscid flux vector $\bar{F}_e(Q)$ are given by

$$Q = \begin{Bmatrix} \rho \\ \rho u \\ \rho v \\ E \end{Bmatrix}, \quad f_e(Q) = \begin{Bmatrix} \rho u \\ \rho u^2 + p \\ \rho uv \\ u(E + p) \end{Bmatrix}, \quad g_e(Q) = \begin{Bmatrix} \rho v \\ \rho uv \\ \rho v^2 + p \\ v(E + p) \end{Bmatrix}. \quad (3.1b)$$

Here ρ is the density, u and v are the velocity components in x and y directions, p is the pressure, and E is the total energy. The pressure is related to the total energy by

$$E = \frac{p}{\gamma - 1} + \frac{1}{2} \rho (u^2 + v^2), \quad (3.1c)$$

with ratio of specific heats γ , which is taken to be 1.4 in all the simulations in this paper. The Cartesian components $f_v(Q, \nabla Q)$ and $g_v(Q, \nabla Q)$ of the viscous flux vector $\bar{F}_v(Q, \nabla Q)$ are given by

$$f_v(Q, \nabla Q) = \mu \cdot \begin{Bmatrix} 0 \\ 2u_x + \lambda(u_x + v_y) \\ v_x + u_y \\ u[2u_x + \lambda(u_x + v_y)] + v(v_x + u_y) + \frac{C_p}{P_r} T_x \end{Bmatrix} \quad (3.1d)$$

$$g_v(Q, \nabla Q) = \mu \cdot \begin{Bmatrix} 0 \\ v_x + u_y \\ 2v_y + \lambda(u_x + v_y) \\ u(v_x + u_y) + v[2v_y + \lambda(u_x + v_y)] + \frac{C_p}{P_r} T_y \end{Bmatrix} \quad (3.1e)$$

where μ is the dynamic viscosity, C_p is the specific heat at constant pressure, P_r is the Prandle number, T is the temperature and using the Stokes hypothesis, $\lambda = -2/3$. Again following the LDG approach, we define the following auxiliary variable,

$$G = \nabla Q. \quad (3.2)$$

Then Eq. (3.1a) becomes

$$\frac{\partial Q}{\partial t} + \nabla \cdot \vec{F}_e(Q) - \nabla \cdot \vec{F}_v(Q, G) = 0. \quad (3.3)$$

Integrating (3.2) and (3.3) in $C_{i,j}$ and performing integration by parts, we obtain

$$\bar{G}_{i,j} V_{i,j} = \sum_{r=1}^K \int_{A_r} Q \mathbf{n} dA \quad (3.4)$$

$$\frac{d\bar{Q}_{i,j}}{dt} + \frac{1}{V_{i,j}} \left(\sum_{r=1}^K \int_{A_r} \vec{F}_e(Q) \cdot \mathbf{n} dA - \sum_{r=1}^K \int_{A_r} \vec{F}_v(Q, G) \cdot \mathbf{n} dA \right) = 0. \quad (3.5)$$

Because Q and G are discontinuous at SV boundaries, the auxiliary flux, inviscid and viscous fluxes are replaced by “numerical fluxes” \hat{Q} , \tilde{F}_e and \tilde{F}_v . The auxiliary and viscous fluxes take the following form

$$\hat{Q} \approx Q^L \quad (3.6)$$

$$\hat{F}_v \approx \tilde{F}_v(Q^L, G^R). \quad (3.7)$$

The inviscid flux \tilde{F}_e used here is the Roe flux splitting²².

IV. Numerical Experiments

A. Accuracy Study with 1D and 2D Convection-Diffusion Equations

Extensive accuracy studies were carried out for both 1D and 2D convection and diffusion equations. In 1D, both linear and non-linear equations are employed, and problems with exact solutions are designed to test the local spectral volume (LSV) approach. These accuracy studies are presented next.

1. 1D Linear Convection-Diffusion Equation

The following linear equation is solved with SV schemes of various orders

$$u_t + u_x - u_{xx} = 0$$

subject to the initial condition of $u(x,0) = \sin(x)$ and periodic boundary condition. The computational domain is $[-\pi, \pi]$. The numerical simulation was carried out until $t=1$. The L_1 and L_∞ errors are presented in Table 1. Note that the LSV approach is capable of achieving the optimum orders of accuracy in all cases.

Table 1. L_1 and L_∞ errors and orders of accuracy for 1D linear equation (at $t = 1.0$)

Order of accuracy	nTCell	L_1 error	L_1 order	L_∞ error	L_∞ order
2	10	7.60e-03	--	9.97e-03	--
	20	2.07e-03	1.88	2.89e-03	1.79
	40	5.46e-04	1.92	7.86e-04	1.88
	80	1.40e-04	1.96	2.04e-04	1.95
3	10	3.83e-04	--	5.37e-04	--
	20	4.55e-05	3.07	6.64e-05	3.02
	40	5.57e-06	3.03	8.16e-06	3.02
	80	6.89e-07	3.02	1.01e-06	3.01
4	10	1.24e-05	--	1.85e-05	--
	20	7.92e-07	3.97	1.17e-06	3.98
	40	5.01e-08	3.98	7.43e-08	3.98
	80	3.15e-09	3.99	4.69e-09	3.99

2. 1D Viscous Burger's Equation

Consider

$$u_t + u \cdot u_x - \mu u_{xx} = 0, \quad \mu = 0.1, \quad x \in (0,1)$$

with the following initial condition $u(x,0) = -\tanh\left(\frac{x}{2\mu}\right)$ and boundary condition

$$u(0,t) = 0, \quad u(1,t) = -\tanh\left(\frac{1}{2\mu}\right).$$

The problem has the following exact solution

$$u(x,t) = -\tanh\left(\frac{x}{2\mu}\right).$$

The simulation is conducted until $t = 1.0$ with various SV schemes. The L_1 and L_∞ errors are presented in Table 2. Note that the LSV approach is again capable of achieving the optimum orders of accuracy in all cases.

Table 2. L_1 and L_∞ errors and orders of accuracy for 1D viscous Burger's equation (at $t = 1.0$)

Order of accuracy	NTCell	L_1 error	L_1 order	L_∞ error	L_∞ order
2	10	2.12e-03	--	1.22e-02	--
	20	6.16e-04	1.78	4.30e-03	1.50
	40	1.73e-04	1.83	1.33e-03	1.69
	80	4.76e-05	1.86	3.66e-04	1.86
3	10	4.84e-04	--	3.43e-03	--
	20	7.62e-05	2.67	5.25e-04	2.71
	40	1.04e-05	2.87	7.06e-05	2.89
	80	1.36e-06	2.93	9.12e-06	2.95
4	10	3.17e-05	--	2.16e-04	--
	20	1.49e-06	4.41	9.53e-06	4.50
	40	7.31e-08	4.35	8.62e-07	3.47
	80	4.22e-09	4.11	6.20e-08	3.80

3. 1D Fully Nonlinear Equation

Further, we consider the following fully nonlinear equation

$$u_t + u \cdot u_x - \frac{1}{2}(u \cdot u_x)_x = 0 \quad x \in (0,1)$$

with initial and boundary conditions as $u(x,0) = e^x$; $u(0,t) = 1$, $u(1,t) = e$. The problem has the following exact solution $u(x,t) = e^x$.

The simulation was conducted until $t = 1.0$ with various SV schemes. The L_1 and L_∞ errors are presented in Table 3. Note that the LSV approach is again capable of achieving the optimum order of accuracy in all cases.

Table 3. L_1 and L_∞ errors and orders of accuracy for the fully nonlinear equation (at $t = 1.0$)

Order of accuracy	nTCell	L_1 error	L_1 order	L_∞ error	L_∞ order
2	10	9.52e-04	--	2.1e-03	--
	20	2.53e-04	1.91	6.12e-04	1.78
	40	6.52e-05	1.96	1.65e-04	1.89
	80	1.65e-05	1.98	4.27e-05	1.95
3	10	9.32e-06	--	2.92e-05	--
	20	1.22e-06	2.93	3.99e-06	2.87
	40	1.56e-07	2.97	5.21e-07	2.94
	80	1.97e-08	2.99	6.65e-08	2.97
4	10	6.30e-08	--	2.37e-07	--
	20	4.07e-09	3.95	1.64e-08	3.85
	40	2.59e-10	3.97	1.07e-09	3.94
	80	1.63e-11	3.99	6.81e-11	3.97

4. 2D Linear Convection and Diffusion Equation

We also tested the LSV method on a 2D linear equation written as

$$u_t + c(u_x + u_y) - \mu(u_{xx} + u_{yy}) = 0, \quad (x, y) \in (-1,1) \times (-1,1); \quad c = 1., \mu = 0.01$$

with the initial condition $u(x, y, 0) = \sin(\pi(x + y))$ and periodic boundary condition. The exact solution is $u(x, y, t) = e^{-2\pi\mu t} \sin(\pi(x + y - 2ct))$. The recorded L_1 and L_∞ errors in Table 4 again show that the LSV approach is capable of achieving the optimum orders of accuracy in all cases.

Table 4. L_1 and L_∞ errors and orders of accuracy for the 2D linear equation (at $t = 1.0$)

Order of accuracy	Grid	L_1 error	L_1 order	L_∞ error	L_∞ order
2	10x10x2	3.73e-02	--	5.35e-02	--
	20x20x2	8.60e-03	2.12	1.28e-02	2.06
	40x40x2	2.16e-03	1.99	3.25e-03	1.98
	80x80x2	5.36e-04	2.01	8.11e-04	2.00
3	10x10x2	2.79e-03	--	3.91e-03	--
	20x20x2	3.40e-04	3.04	5.10e-04	2.94
	40x40x2	4.16e-05	3.03	6.31e-05	3.01
	80x80x2	5.21e-06	3.00	7.97e-06	2.98
4	10x10x2	4.14e-05	--	5.72e-05	--
	20x20x2	2.47e-06	4.07	3.37e-06	4.09
	40x40x2	1.47e-07	4.07	1.95e-07	4.11
	80x80x2	8.45e-09	4.12	1.14e-08	4.10

B. Accuracy Study for the Navier-Stokes Equations

To evaluate the formal order of accuracy of the local SV method for the Navier-Stokes equations, we employ the compressible Couette flow between two parallel walls, which has an analytical solution. The lower wall is stationary with temperature T_0 and the upper wall is moving at speed of U with temperature T_1 . The distance between the two walls is H . The steady analytic solution is

$$u = \frac{U}{H} y, \quad v = 0,$$

$$p = \text{const } t, \quad \rho = \frac{p}{R \cdot T},$$

$$T = T_0 + \frac{y}{H} \cdot (T_1 - T_0) + \frac{\mu \cdot U^2}{2k} \cdot \frac{y}{H} \cdot \left(1 - \frac{y}{H}\right).$$

The following parameters are chosen

$$U = 1, H = 2, T_0 = 0.8, T_1 = 0.85, \mu = 0.01.$$

The computational domain was selected to be $[0,2] \times [0,2]$. The simulation was started with the following initial condition:

$$u = 0, v = 0, p = 1, T = 1.$$

Convergence is assumed when the residual drops by 6 orders of magnitude. Figure 2 shows a typical convergence history for velocity and temperature. A sequence of regular triangular meshes was used to perform a grid-refinement accuracy study. The L_1 and L_∞ density errors computed with 2nd, 3rd and 4th order SV schemes on these meshes are presented in Table 5. Note that 2nd and 4th order SV schemes can achieve the formal order of accuracy in the L_1 norm, while the 3rd order SV scheme showed sub-optimal order of accuracy. It is suspected that the partition for the quadratic SV has too large a Lebesgue constant. We plan to further optimize this SV. The L_∞ order all showed some deterioration. We plan to carry out further investigation to understand why.

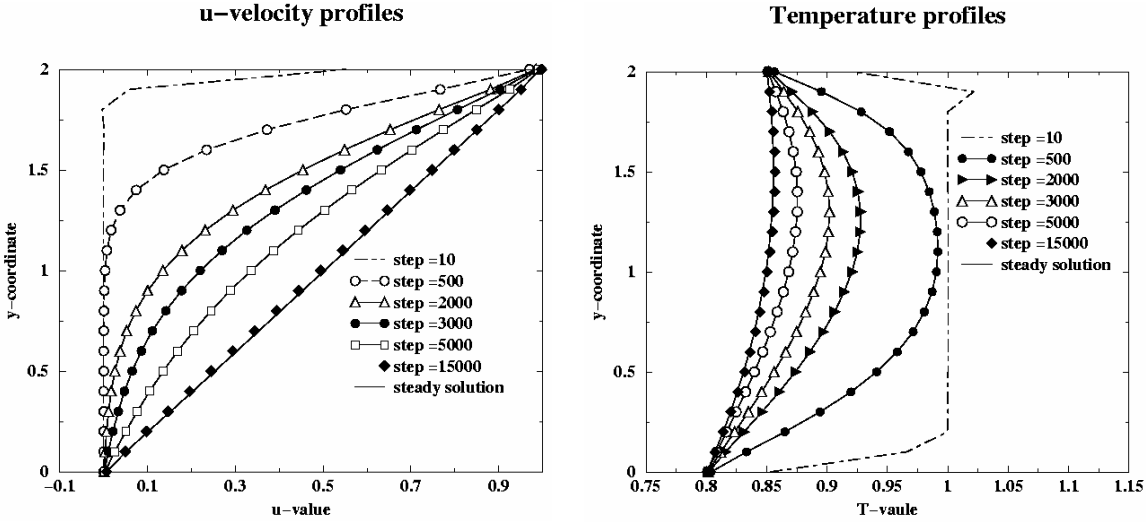


Figure 2. Convergence histories of numerical solution to the steady exact solution

Table 5. L_1 and L_∞ density errors and orders of accuracy for the Couette flow

Order of accuracy	Grid	L_1 error	L_1 order	L_∞ error	L_∞ order
2	10x10x2	1.28e-04	---	3.31e-04	---
	20x20x2	3.35e-05	1.93	8.82e-05	1.91
	40x40x2	1.04e-05	1.69	2.55e-05	1.79
	80x80x2	3.79e-06	1.45	8.09e-06	1.65
3	10x10x2	6.74e-07	---	4.29e-06	---
	20x20x2	1.30e-07	2.38	8.22e-07	2.38
	40x40x2	2.62e-08	2.31	1.94e-07	2.08
	80x80x2	5.88e-09	2.16	5.32e-08	1.87
4	10x10x2	2.27e-08	---	7.09e-08	---
	20x20x2	1.32e-09	4.10	4.17e-09	4.09
	40x40x2	7.43e-11	4.15	3.80e-10	3.46
	80x80x2	5.00e-12	3.89	4.68e-11	3.02

C. Laminar Flow over a Flat Plate

Next we consider the laminar flow on an adiabatic flat plate characterized by a free stream Mach number $M = 0.3$ and by a Reynolds number based on the free stream condition and the plate length $Re = 500$. The computational domain is selected to be $[-0.5, 1.5] \times [0, 4]$ and the leading edge starts at $x = 0$. Three triangular meshes generated from structured grids were used in the simulation to demonstrate grid convergence, as shown in Figure 3. The coarsest mesh has $13 \times 11 \times 2$ cells with 8 cells along the flat plate. Uniform refinement was then used to obtain the medium and fine meshes. We present results obtained with linear, quadratic, and cubic reconstructions and compare

the computed skin friction coefficient (C_f) with the well-known incompressible Blasius formula along the flat plate in Figure 4(a-c). The computed results show a good agreement with the Blasius solution.

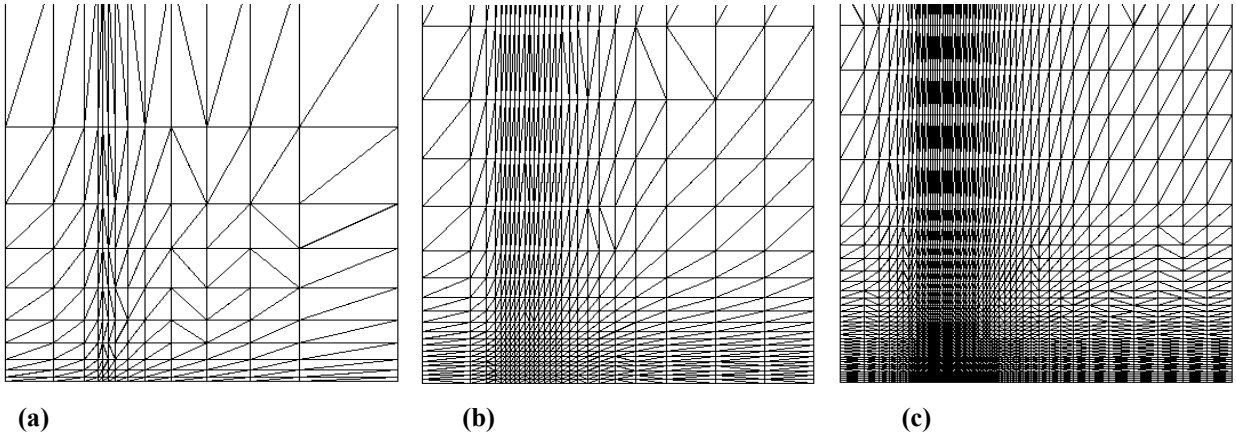


Figure 3. Three different meshes (a) coarse, (b) medium, (c) fine

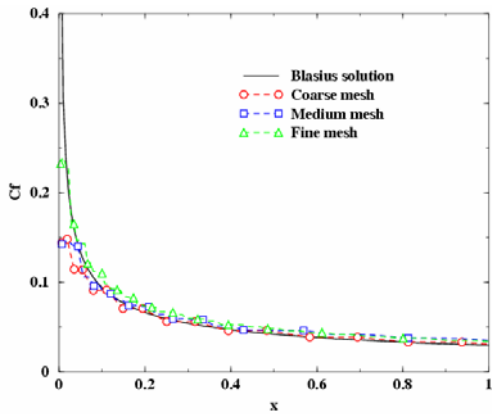


Figure 4a. Comparison of skin friction coefficients computed using linear reconstruction

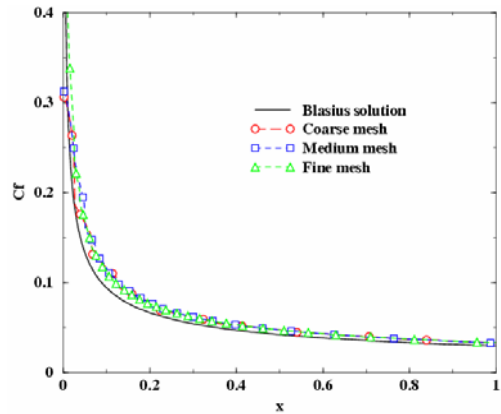


Figure 4b. Comparison of skin friction coefficients computed using quadratic reconstruction

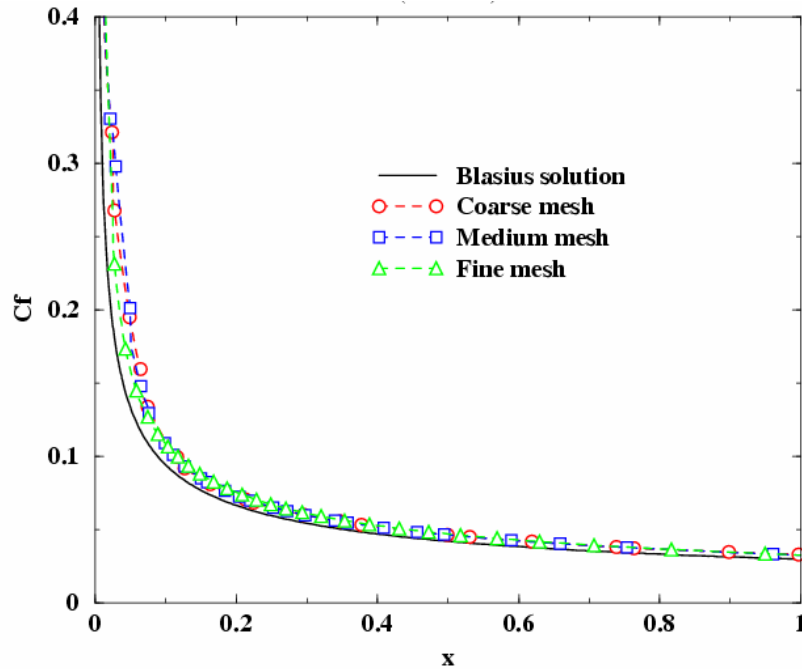


Figure 4c. Comparison of skin friction coefficients computed using cubic reconstruction

V. Conclusions and Future Work

The SV method is successfully extended to the Navier-Stokes equations by following a mixed formulation named the local discontinuous Galerkin approach originally developed for the DG method. The approach, which is named the local SV (LSV) approach, is tested extensively for 1D and 2D convection-diffusion equations using a series of accuracy studies. All tests indicated that the formulation is capable of achieving the formal optimum order of accuracy in both the L_1 and L_∞ norms. The LSV approach is then implemented and tested for the Navier-Stokes equations, and was able to achieve the formal order of accuracy for the compressible Couette flow problem. The case of laminar flow over a flat plate was simulated successfully with good agreement with the Blasius solution.

We plan to test the SV solver for more complex viscous flow problems, and develop an implicit version to speed up the convergence rate to steady state.

References

- ¹Z.J. Wang, "Spectral (finite) volume method for conservation laws on unstructured grids: basic formulation", *J. Comput. Phys.* Vol. 178, 2002, pp. 210-251.
- ²Wang, Z.J. and Liu, Yen, "Spectral (Finite) Volume Method for Conservation Laws on Unstructured Grids II: Extension to Two-Dimensional Scalar Equation", *J. Comput. Physics*, Vol. 179, 2002, pp. 665-697.
- ³Z.J. Wang and Yen Liu, "Spectral (finite) volume method for conservation laws on unstructured grids III: one-dimensional systems and partition optimization," *Journal of Scientific Computing*, Vol. 20, 2004, pp.137-157.
- ⁴Z.J. Wang, L. Zhang and Y. Liu, "Spectral (Finite) Volume Method for Conservation Laws on Unstructured Grids IV: Extension to Two-Dimensional Euler Equations," *J. Comput. Phys.* Vol. 194, 2004, pp. 716-741.
- ⁵S.K. Godunov, "A finite-difference method for the numerical computation of discontinuous solutions of the equations of fluid dynamics," *Mat. Sb.* Vol. 47, 1959, pp. 271.
- ⁶B. Cockburn, S. -Y. Lin and C. -W. Shu, "TVD Runge-Kutta local projection discontinuous Galerkin finite element method for conservation laws III: one-dimensional systems," *J. Comput. Phys.* Vol. 84, 1989, pp. 90-113.
- ⁷T. J. Barth and P.O. Frederickson, "High-order solution of the Euler equations on unstructured grids using quadratic reconstruction," *ALAA Paper*, No. 90-0013, 1990.
- ⁸G. Jiang and C. -W. Shu, "Efficient implementation of weighted ENO," *J. Comput. Phys.* Vol. 126, 1996, pp. 202.
- ⁹X.D. Liu, S. Osher and T. Chan, "Weighted essentially non-oscillatory schemes," *J. Comput. Phys.* Vol. 115, 1994, pp. 200-212.

- ¹⁰C. -W. Shu, "Essentially non-oscillatory and weighted essentially non-oscillatory schemes for hyperbolic conservation laws," *In Advanced Numerical Approximation of Nonlinear Hyperbolic Equations*, B. Cockburn, C. Johnson, C. -W. Shu and E. Tadmor (Editor: A Quarteroni), Lecture Notes in Mathematics, volume , Springer, 1697, 1998; pp.325-432.
- ¹¹Yuzhi Sun and Z.J.Wang, "Evaluation of discontinuous Galerkin and spectral volume methods for scalar and system conservation laws on unstructured grids," *International journal for numerical methods in fluids*, in press.
- ¹²M. Zhang and C. -W. Shu, "An analysis of and a comparison between the discontinuous Galerkin and spectral finite volume method," *Computers and Fluids*, to appear.
- ¹³B. Cockburn and C. -W. Shu, "The local discontinuous Galerkin method for time-dependent convection diffusion system," *SIAM J. Numer. Anal.* Vol. 35, 1998, pp. 2440-2463.
- ¹⁴F. Bassi and S. Rebay, "A high-order accurate discontinuous finite element method for the numerical solution of the compressible Navier-Stokes equations," *J. Comput. Phys.* Vol. 131, 1997, pp. 267-279.
- ¹⁵C. E. Baumann and J.T. Oden, "A discontinuous *hp* finite element method for convection-diffusion problems," *Comput. Methods Appl. Mech. Engrg.* Vol. 175, 1999, pp. 311-341.
- ¹⁶J.T. Oden, Ivo Babuska, and C.E. Baumann, "A discontinuous *hp* finite element method for diffusion problems," *J. Comput. Phys.*, Vol. 146, 1998, pp. 491-519.
- ¹⁷B. Riviere, M. Wheeler and V. Girault, "A priori error estimates for finite element methods based on discontinuous approximation spaces for elliptic problems," *SIAM J. Numer. Anal.* Vol. 39, 2001, pp. 902-931.
- ¹⁸C. -W. Shu, "Different formulations of the discontinuous Galerkin method for the viscous terms," *In Advances in Scientific Computing*, Z. -C. Shi, M. Mu, W. Xue and J. Zou, editors, Science Press, 2001; pp. 144-145.
- ¹⁹M. Zhang and C. -W. Shu, "An analysis of three different formulations of the discontinuous Galerkin method for diffusion equations," *Mathematical Models and Methods in Applied Sciences*, Vol. 13, 2003, pp.395-413.
- ²⁰Yuzhi Sun and Z.J. Wang, "Formulations and analysis of the spectral volume method for the diffusion equation," *Communications in Numerical Methods in Engineering*, accepted.
- ²¹Paul Castillo, "An optimal estimate for the local discontinuous Galerkin method, in Discontinuous Galerkin methods", edited by B. Cockburn, G.E. Karniadakis, and C.-W. Shu, *Lecture Notes in Computational Science and Engineering*, Springer, 11, 2000, pp. 285-290.
- ²²P.L. Roe, "Approximate Riemann solvers, parameter vectors, and difference schemes," *J. Comput. Phys.* Vol. 43, 1981, pp. 357-372.